*29th EPS Conference on Plasma Phys. and Contr. Fusion Montreux, 17-21 June 2002 ECA Vol. **26B**, P-2.067 (2002)*

Turbulence Measurements on DIII-D Discharges with Modulated ECH and Comparisons with Turbulence Simulations

R. V. Bravenec,[1] D. W. Ross,[1] G. R. McKee,[2] J. C. DeBoo,[3] W. Dorland,[4] M. E. Austin,[1] K. W. Gentle,[1] T. L. Rhodes,[5] L. Zeng,[5] and the DIII-D Team[3]

[1]*Fusion Research Center, The University of Texas, Austin, Texas, USA*
[2]*University of Wisconsin, Madison, Wisconsin, USA*
[3]*General Atomics, San Diego, California, USA*
[4]*Imperial College, London, England*
[5]*University of California, Los Angeles, California, USA*

Introduction

Earlier, density fluctuations measured with beam-emission spectroscopy (BES) and energy transport in the DIII-D tokamak were compared to gyrofluid simulations by the nonlinear GRYFFIN code [1]. Here we extend this work to plasma perturbations by modulated off-axis electron-cyclotron heating (ECH), to predictions of the nonlinear gyrokinetic code GS2 [2], and to inclusion of fluctuation measurements by FIR scattering and reflectometry.

Experimental results

To avoid edge-localized modes (ELMs) and sawteeth, an inner-wall-limited L-mode plasma with early neutral-beam heating was utilized [3]. The ECH antenna orientation considered here produced second-harmonic (110 GHz) X-mode heating at a flux-surface radius $\rho \equiv r/a \approx 0.815$ (FWHM ≈ 0.057). The ECH waveform was approximately square-wave with a 40-ms period and ~50% duty cycle. The BES system [4] consisted of 30 sight-lines ("channels") of ~1 cm focal diameter distributed in a 6 (horizontal) × 5 (vertical) array spaced by ~1 cm. These were located just below the plasma midplane and interior to the ECH-resonance flux surface.

To improve the statistics, 1-MHz fluctuation data from twelve 8-ms bins separated by the ECH modulation period were grouped into individual data sets representing a particular phase of the modulation. To further enhance the signal-to-noise, the fluctuation levels were derived from the cross powers between vertically adjacent channels since electronics and photon noise decorrelate. The cross-power spectra peak at $f_0 \approx 150$ kHz at the inner vertical array and at ~100 kHz at the outer vertical array and are broad (FWHM $\approx f_0$) above ~50 kHz.

The fluctuation levels from the six vertical arrays, obtained from the square roots of the cross powers integrated between 50 and 300 kHz and suitably normalized, are shown in Fig. 1 at 4-ms steps through an "average" ECH cycle. Data for each array (labeled by their *r/a* location) are represented by an average over adjacent pairs of channels. The corresponding density fluctuation levels ($\tilde{n}/n$) are obtained by correcting for the saturation of the n=3 state with density [5] and finite collection area and correlation lengths [6]. The time-averaged $\tilde{n}/n$ at the inner and outer arrays are ~0.9 % and ~1.35 %, respectively.

The fluctuations are slightly (~3%) but clearly modulated by the ECH and are approximately out of phase (drop at ECH turn-on, rise at ECH turn-off). Both a reflectometer channel near $\rho \approx 0.9$ and FIR scattering at $k_\theta \sim 1$ cm^{-1} observe a modulation of fluctuation level approximately *in phase* with the ECH. This apparent discrepancy will be addressed later.

The poloidal velocity of the fluctuations v_θ is computed at each vertical array from time-delay correlation between the top and bottom channels. Unlike the fluctuation levels, no modulation of the velocities is evident. The poloidal velocities at the inner and outer arrays (corrected for finite collection area) are ~9.6 km/s and ~8.0 km/s, respectively. (Positive velocities denote ion diamagnetic direction.) The normalized mean poloidal wave numbers $\bar{k}_\theta \rho_i$, obtained from the cross-phase spectrum evaluated at f_0 and corrected for finite collection area, are ~0.29 and ~0.26, respectively.

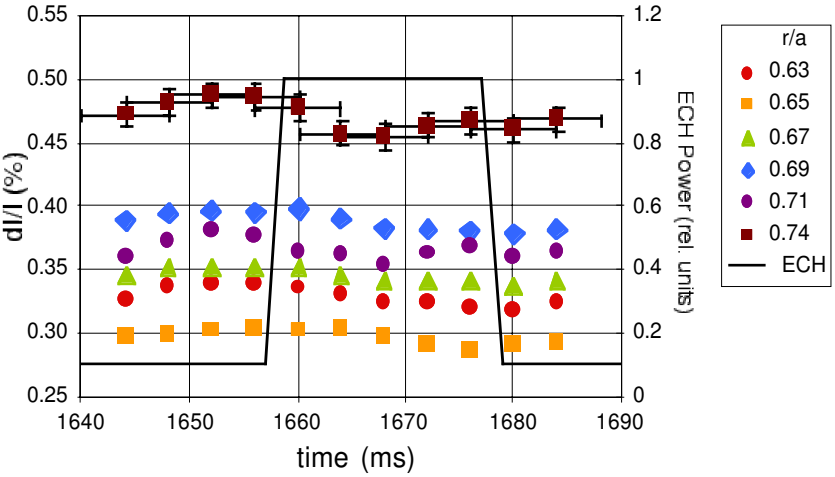

Fig. 1. Emission-intensity fluctuation levels for the six BES poloidal arrays during an ECH cycle.

Correlations between modulations of fluctuations and plasma profiles

Time-dependent profile data was obtained only for the electron temperature T_e from electron-cyclotron emission (ECE). Shown in Fig. 2 are $T_e(t)$ and $dT_e(t)/dr$ for an average ECH period. As expected, T_e rises and equilibrates [3] quickly during the ECH pulse for $\rho \geq 0.7$, whereas the gradient slightly flattens interior to the ECH resonance (r/a = 0.815), remains roughly constant (except for transients) at the resonance location, and steepens outside. (The scale length $L_{Te} \equiv T_e/|dT_e/dr|$ increases everywhere during the ECH pulse.) The phase of the fluctuation modulation shown in Fig. 1 is consistent with dT_e/dr acting as a drive of the turbulence. The opposite phase of dT_e/dr outside the ECH resonance could explain the phases observed by the edge reflectometry channel and scattering. ($\tilde{n}$ peaks near the plasma edge and scattering at low wave numbers is effectively a chord-averaged measurement.)

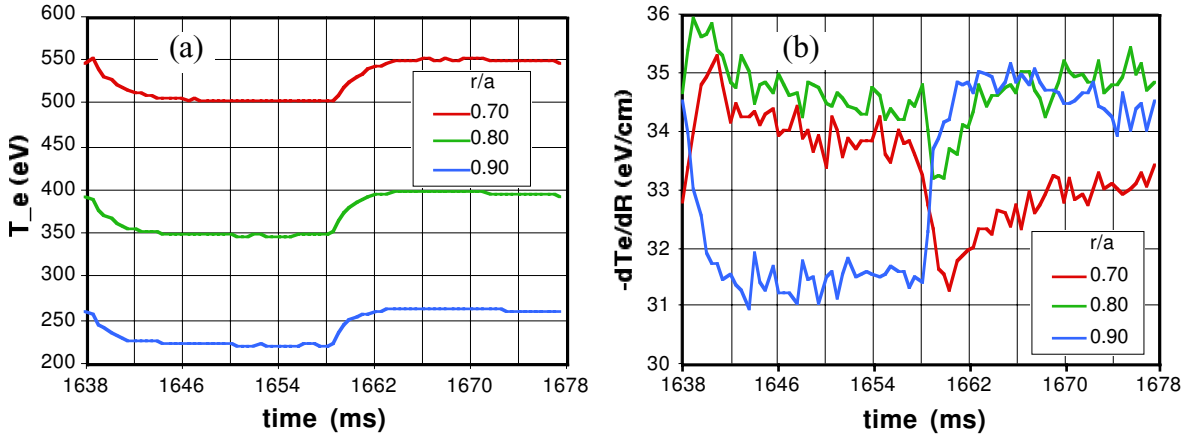

Fig. 2. (a) Electron temperature and (b) radial gradient boxcar-averaged over 17 ECH periods. The ECH resonance is centered at $r/a \approx 0.815$.

Gyrofluid and gyrokinetic simulations of the time-averaged discharge

We have carried out linear and nonlinear gyrofluid [7] and gyrokinetic [2] flux-tube simulations with plasma parameters corresponding to $r/a = 0.7$. From linear simulations, the turbulence is dominated by ion-temperature-gradient (ITG) modes at $k_\theta \rho_i \leq 1$ and electron-temperature-gradient (ETG) modes for $k_\theta \rho_i \geq 1$. Since the fluctuation diagnostics cannot observe them and the codes do not include them, we ignore ETG modes in the following. (If present, they would manifest themselves in the measured power fluxes, however.) The growth rate is positive for $0 \leq k_\theta \rho_i \leq 1$, peaking at $\bar{k}_\theta \rho_i \sim 0.6$ with a value of $\gamma_{max} \sim 60$ krad/s, about the same as the real frequency. The poloidal phase velocity is $\omega/k_\theta \sim 0.3 v_i^* \sim 0.18$ km/sec, where v_i^* is the ion diamagnetic velocity. Currently not included in the codes is the background $\boldsymbol{E}\times\boldsymbol{B}$ flow shear. As a rule of thumb [8], γ_{max}, fluxes, and $(\tilde{n}/n)^2$ are reduced by roughly the factor $(1 - \omega_{E\times B}/\gamma_{max})$, where $\omega_{E\times B} \equiv (RB_\theta)^2/B\ \partial(E_r/RB_\theta)/\partial\psi$ (ψ being the flux function) [9]. We neglect this factor since the estimated $\omega_{E\times B} \approx 7.9 \pm 13$ krad/s (outboard side, less inboard) is smaller than $\gamma_{max} \sim 60$ krad/s (although the uncertainties are large).

The measured input profiles were adjusted within their error bars to seek agreement with the measured ion and electron power fluxes P_e and P_i, and $\tilde{n}/n$. The error bars were especially large for $\hat{s} \equiv \rho/q\,(dq/d\rho)$, E_r, and $\omega_{E\times B}$ since they weren't measured for the specific discharge considered here. Since E_r and $\omega_{E\times B}$ do not appear explicitly in the codes, we varied $\hat{s}$ and $L_{Ti} \equiv T_i/|dT_i/dr|$. As expected, P_e, P_i, and $\tilde{n}/n$ increase as R/L_{Ti} increases or $\hat{s}$ decreases. P_e and P_i are most sensitive to $\hat{s}$ and R/L_{Ti}, respectively, while $\tilde{n}/n$ is generally less sensitive.

These and other parameters for our best simulations of the time-averaged discharge are listed in Table I in the top row for each code. Although we did not exactly match the experimental values of P_e, P_i, and $\tilde{n}/n$, it may be possible with enough computer time and by exploiting the experimental uncertainties in so many relevant parameters. We see that GRYFFIN underestimates P_e while overestimating $\tilde{n}/n$: a combination that may be hard to rectify. Both codes give marginally larger values of $\bar{k}_\theta \rho_i$ than measured. The serious discrepancies in v_θ are most likely due to additional uncertainties in the poloidal $\boldsymbol{E}\times\boldsymbol{B}$ velocity E_r/B_T estimated from charge-exchange recombination spectroscopy as 2.0 ± 0.5 km/s at $r/a = 0.7$ (3.4 ± 0.7 km/sec at $r/a = 0.8$), which was subtracted from the measured velocity.

Gyrofluid and gyrokinetic simulations of the ECH modulations

We simulate the ECH modulation by changing T_e and L_{Te}, guided by Fig. 2. The nonlinear runs saturate in much less than an ECH period, so the turbulence should respond almost instantaneously to profile changes induced by the modulated ECH. To investigate the effects of T_e and L_{Te} alone, we increase each by 10-20% in separate runs. The results for each code are listed in Table I. For GS2 each perturbation alone slightly reduces $\tilde{n}/n$ (although within the error bars), in agreement with the BES data (assuming the combination does likewise). For GRYFFIN, the perturbations either have no effect or increase $\tilde{n}/n$.

Conclusions

These results are by no means definitive, since the time-averaged simulations did not exactly

match the experiment, nor did we establish uniqueness, *i.e.*, if some other combination of input profiles could produce the same simulation results. Future work will aim to vary other profiles such as $n_e(r)$, $Z_{eff}(r)$, *etc.* and to include $\boldsymbol{E}\times\boldsymbol{B}$ flow shear. We will also consider the possible modulation of plasma profiles other than $T_e(r)$ and compare simulated and measured modulations of the power fluxes.

	R/L_{Ti}	R/L_{Te}	T_e/T_i	$\hat{s}$	P_i (MW)	P_e (MW)	$\tilde{n}/n$ (%)	$\bar{k}_\theta\rho_i$	v_θ (km/s)
Exp.	4.3±1.3	7.2±0.2	0.95±0.05	1.3±0.5	1.54	1.67	0.91	0.29	7.6 ± 0.6
GS2	5.0	7.18	0.95	1.50	1.42	2.10	1.08	0.33	< 0.19
	"	5.70	"	"	1.42	1.47	1.02	~0.33	"
	"	7.18	1.14	"	1.52	2.61	1.02	~0.33	"
Gryffin	6.1	7.18	0.95	1.87	1.48	0.76	1.55	0.40	< 0.17
	"	6.46	"	"	1.50	0.70	1.54	0.35	"
	"	7.18	1.05	"	1.52	0.87	1.75	0.35	"

Table I. Measured and simulated time-averaged electron and ion power fluxes, density fluctuation level, mean normalized poloidal wave number, and poloidal group velocity (in frame with $E_r = 0$) at $r/a = 0.7$.

Acknowledgments

The authors wish to thank the DIII-D operations and diagnostics staff. This work was supported by USDOE under contracts DE-AC03-99ER54463 and DE-AC05-00OR22725, and grants DE-FG03-97ER54415, DE-FG03-95ER54296, DE-FG02-89ER53296, and DE-FG03-01ER54615.

References

[1] R. V. Bravenec, D. W. Ross, G. R. McKee, *et al.*, in *Proc. of 25th EPS Conf. on Controlled Fusion and Plasma Phys.*, Prague (European Physical Society, Petit-Lancy, Switzerland, 1998), Vol. 22C, p. 802, 1998.

[2] W. Dorland, F. Jenko, M. Kotschenreuther, and B. N. Rogers, Phys. Rev. Lett. **85**, 5579 (2000); F. Jenko, W. Dorland, M. Kotschenreuther, and B. N. Rogers, Phys. Plasmas **7**, 1904 (2000); M. Kotschenreuther, G. Rewoldt, and W. M. Tang., Comput. Phys. Commun. **88**, 128 (1995).

[3] J. C. DeBoo, M. E. Austin, R. V. Bravenec, J. E. Kinsey, J. Lohr, T. C. Luce, G. R. McKee, C. C. Petty, R. Prater, T. L. Rhodes, G. M. Staebler, L. Zeng, these proceedings.

[4] G. McKee, R. Ashley, R. Durst, R. Fonck, M. Jakubowski, K. Tritz, K. Burrell, C. Greenfield, and J. Robinson, Rev. Sci. Instrum. **70**, 913 (1999); **70**, 2179(E) (1999).

[5] R. J. Fonck, P. A. Duperrex, and S. F. Paul, Rev. Sci. Instrum. **61**, 3487 (1990).

[6] R. V. Bravenec, in *Transport, Chaos and Plasma Physics 2*, edited by S. Benkadda, F. Doveil, Y. Elskens, (World Scientific, New Jersey, 1996), pp. 350-357.

[7] M. A. Beer, Ph.D. thesis, Princeton University (1995); M. A. Beer, S. C. Cowley, and G. W. Hammett, Phys. Plasmas **2**, 2687 (1995).

[8] R. E. Waltz, R. L. Dewar, and X. Garbet, Phys. Plasmas **5**, 1784 (1998).

[9] T. S. Hahm and K. H. Burrell, Phys. Plasmas **2**, 1648 (1995).